doi:10.1246/cl.2012.562

Published on the web May 19, 2012

Highlight Review

New Synthetic Opportunities in Miniaturized Flow Reactors with Inductive Heating

Andreas Kirschning,* Lukas Kupracz, and Jan Hartwig

(Received March 7, 2012; CL-120196)

Abstract

Inductive heating has emerged as a new heating technique in the laboratory, particularly when combined with miniaturized flow reactor devices. Traditionally, inductive heating is found in industrial applications like the heating of large metallic objects such as in the bending of pipes, bonding and welding. New fields of application are the preparation of nanotubes as well as hyperthermia in the treatment of cancer. This account specifically addresses the use of heatable materials such as superparamagnetic iron oxide nanoparticles in many areas of organic synthesis and how this enabling technology compares to conventional as well as microwave heating.

♦ Introduction

Over the last decades inductive heating has developed into a widely used method for various applications in chemistry, manufacturing, and medicine. Compared to conventional or microwave heating[1] it provides several advantages. Technically, the system is easy to set up consisting of an induction coil and an alternating current generator (AC-generator). The material to be heated is commonly located within the magnetic field and therefore no contact to another surface is required. Due to the creation of heat within the material less energy is lost by convection or thermal radiation. Therefore, the energy transfer is more effective at least compared to conventional heating (Table 1).

This benefit of inductive heating allows very rapid heating and cooling of the material saving time and making handling of the workpiece easier.

So far, the technique has mostly been employed for the heating of large metallic objects and workpieces. Inductive heating is also applied for bending of pipes, bonding, welding, sintering, and annealing of metals and alloys.[3] Furthermore, it is used for large-scale melting steel, glass, or silicon.[4] More recently, inductive heating has been also utilized for gluing, heating rubber, forming plastic, or shrinking workpieces.[5] In general, the benefits of this technique are successfully utilized in industrial applications.

Table 1. Power transmission of different heating processes[2]

Heating	Power transmission/$W\,cm^{-2}$
Convection	0.5
Irradiation	8
Heat conduction	20
Flame	1000
Inductive heating	30000

♦ Theoretical Background of Electromagnetic Induction

Materials inside a magnetic field of strength H do influence the magnetic flux density B. The magnetic induction is given by eq 1:

$$B = \mu_0(H + M) \quad (1)$$

where μ_0 is the permeability in vacuum and M the magnetization of the material. In consideration of the relative permeability μ_r the magnetic flux density B is described by eq 2.

$$B = \mu_0\mu_r H \quad (2)$$

The relative permeability characterizes the influence of a material on a magnetic field and depends on the specific properties of the material. In relation to their properties in a magnetic field, materials can be classified as follows: a) Materials with $\mu_r < 1$ are diamagnetic. These materials like copper, silver, or bismuth degrade the magnetic field. b) Materials like aluminium or oxygen with $\mu_r > 1$ are paramagnetic. Both materials display magnetism only in the presence of an applied field. c) As opposed to paramagnetic materials ferromagnetic materials such as crystal modifications of iron, cobalt, and nickel, exhibit strong magnetism ($\mu_r \gg 1$). They preserve magnetization after being exposed to a magnetic field (remanence). The relative permeability μ_r is a function of the magnetic flux density B ($\mu_r = f(B)$) and the ferromagnetic properties disappear after exceeding the Curie temperature T_C (Table 2).

The theoretical principles of inductive heating are based on the effects of oscillating magnetic fields. Oscillating magnetic fields are created if a conductor is connected to an AC-source.

Table 2. Curie temperature for different substances[6]

Material	Curie temperature T_C/°C
Cobalt	1130
Iron	770
Iron oxide	622
Nickel	358

Prof. Andreas Kirschning, Mr. Lukas Kupracz, and Mr. Jan Hartwig*
Institut für Organische Chemie und Biomolekulares Wirkstoffzentrum (BMWZ), Leibniz Universität Hannover, Schneiderberg 1B, 30167 Hannover, Germany
E-mail: Andreas.Kirschning@oci.uni-hannover.de

Under these conditions, different effects are responsible that lead to heating the material:

Joule's heating: The first effect is caused by eddy currents. If an electroconductive material is placed in an oscillating magnetic field, a current will be induced in this conductor which is called eddy current. This induced current leads to a resistor heating called Joule's heating Q where R is the resistor of the electroconductive material (eq 3).

$$Q = I^2 Rt \tag{3}$$

$$P_{\mathrm{ind}} = \frac{{u_{\mathrm{ind}}}^2}{R} = \frac{(2\pi f \mu HA)^2}{R} \tag{4}$$

The inductive power P_{ind} which is an important factor in inductive heating, determines the efficacy of the electric power transformation and is inversely dependant to R (eq 4). f is the frequency of the alternating magnetic field in [Hz] and A the surface of the material. For nonmagnetic conductors like copper or aluminum the Joule's heating is the exclusive mechanism of heating. Additionally, Lenz's law says that the induced current creates a magnetic field which acts in the opposite direction of the inducing field and thus the induced current. Consequently, this phenomenon results in an attenuation of the magnetic field inside the material. It needs to be noted that the eddy current flows on the surface and only this area is heated.

The current density J in a conductor decreases exponentially from its value at the surface J_{s} according to the depth d from the surface (eq 5).

$$J = J_{\mathrm{s}} \exp(d/\delta) \tag{5}$$

$$\delta = \sqrt{\frac{\rho}{\pi \mu_{\mathrm{r}} f}} \tag{6}$$

Here, δ is called skin depth and is given by eq 6 where ρ is the specific resistor of the conductor. This effect is called skin-effect and occurs especially at high frequencies f (Figure 1). Since the specific resistor and the permeability depend on the temperature, the skin depth is not constant; it increases with higher temperature.

Hysteresis: The second effect is caused by magnetic properties of ferromagnetic materials in which magnetic dipoles of the Weiss domains are randomly directed (Figure 2). When placing the ferromagnetic material inside a magnetic field, more and more Weiss domains are in line with the field the stronger the external field is. When the oscillating magnetic field changes direction, the dipoles in the ferromagnetic material are opposed to the field. This results in a higher energy state. By inverting the dipoles they fall back to the lower energy state and the energy difference is converted into thermal energy. In ferromagnetic materials there is no direct correlation between M and H and the hysteresis loss is proportional to area A between the hysteresis curves. It is given by

$$A = f \int M \mathrm{d}H \tag{7}$$

The eddy current loss increases with the square of the frequency. Consequently, the hysteresis is insignificant at high frequencies. However, hysteresis is of relevance below the Curie temperature in ferromagnetic materials.

Brown and Néel relaxation: With decreasing particle size of ferromagnetic materials the formation of multiple Weiss

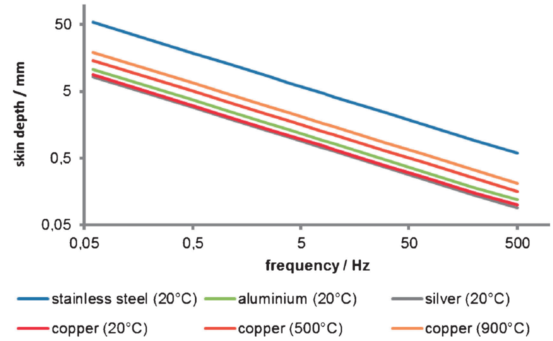

Figure 1. Skin depth as a function of the frequency.[7]

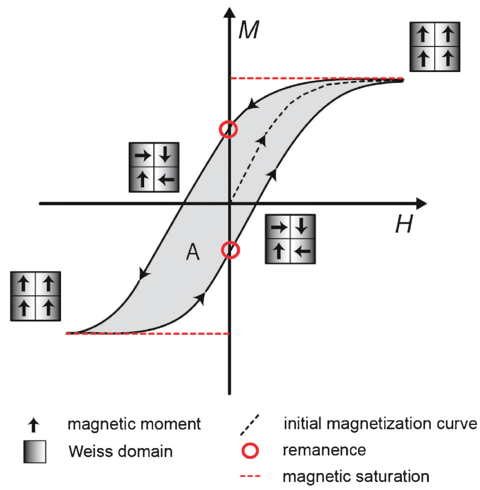

Figure 2. Electric displacement field of a ferromagnetic material.

domains becomes energetically unfavorable. Consequently, below a critical volume domain walls do not exist anymore and the nanoparticles are single domains with a single magnetic moment. The anisotropy energy is smaller than the thermal energy ($KV_{\mathrm{m}} < k_{\mathrm{B}}T$) and consequently thermal fluctuations lead to relaxation phenomena. This phenomenon is called superparamagnetism. It occurs with particle diameters below 3–50 nm, depending on the materials.[8] Superparamagnetic materials possess neither remanent magnetization nor hysteresis (Figure 3).

However, the values of magnetic susceptibility are comparable to ferromagnetic materials.[9] The heat dissipation in a magnetic field is caused by the relaxation of the magnetic moments. It is discriminated between Néel and Brown relaxation.[10] With the Néel mechanism of relaxation the magnetic moment rotates within the crystal. In contrast to the Brown relaxation, the magnetic moment is locked to the crystal axis and the particle rotates with the magnetic moment. The Néel relaxation time τ_{N} depends on the anisotropic energy and the thermal energy (eq 8).

$$\tau_{\mathrm{N}} = \exp(KV_{\mathrm{m}}/k_{\mathrm{B}}T) \tag{8}$$

K is the anisotropy constant, V_{m} the particle volume, and k_{B} the Boltzmann constant. The Brown relaxation time τ_{B} is given by eq 9.

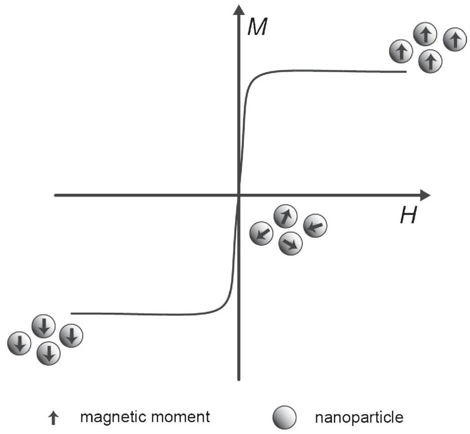

Figure 3. Illustration of superparamagnetic nanoparticles in a magnetic field.

$$\tau_B = \frac{3V_{hyd}}{k_B T}\eta \tag{9}$$

Here, η describes the viscosity and V_{hyd} the hydrodynamic particle volume. From the equations above follows the effective relaxation time τ_{eff} described in eq 10.

$$\tau_{eff} = \frac{\tau_B \tau_N}{\tau_B + \tau_N} \tag{10}$$

Which one of the two mechanisms dominates is governed by the particle size, the particle composition, and the viscosity of the medium.[11] Also a dependency with the frequencies and heating power was encountered.

Rosensweig calculated the power loss P_{nano} of nanoferrite (nanoparticles of iron) as follows:[12]

$$P_{nano} = \mu_0 \pi \chi_0 {H_0}^2 \frac{2\pi f \tau_{eff}}{1 + (2\pi f \tau_{eff})^2} \tag{11}$$

χ_0 is the equilibrium susceptibility and is redundant with the permeability. Thus the heating of the nanoparticles can be controlled by the frequency (f) and amplitude (H) of the external field. Among the composition of the particles the heating behavior is dependent on the particle size and the degree of polydispersion. Low polydispersity, which is governed by the radius of the particles, shows the best heating behavior which[12] renders rather complex heating behavior.

♦ Current Applications

The Production of Carbon Nanotubes.

An important example of a chemical application for inductive heating is the production of carbon nanotubes.[13] Since the discovery of carbon nanotubes (CNTs) in 1991 various methods of preparation have been developed.[14] So far chemical vapor deposition (CVD) or alternatively catalytic chemical vapor deposition (CCVD) introduced by Li et al. in 1996 are the most promising ones, because they allow fairly low energy consumption.[15,16] They are based on the decomposition of a gaseous carbon source on the surface of a metallic catalyst forming carbon nanotubes. In most cases, the catalyst is applied on an inorganic carrier, the so called "suspector," a term introduced by Gennet et al.[17] Various carrier materials such as TiO_2, Fe, Si, or Mo and even $CaCO_3$, silica gel or zeolites have been tested.[13,18,19] It was shown that a porous surface is an excellent support in catalytic nanotube production in terms of adherence, thermal heat conductivity and CNT quality.[20] Catalysts such as Fe, Co, Pd, or Ni can be used elementally, as multilayers, salts or as alloys. The catalyst-doped carrier is heated and a mixture of acetylene or ethylene with nitrogen or hydrogen gas passes along the catalyst to form the CNTs.

There are two common approaches for the CCVD method; these are thermal heating and plasma-enhanced heating. One main advantage of thermal heating is the opportunity to carefully control the conditions for generating single- or multiwalled CNTs with desired diameters. This method requires heating the whole reactor and nondirected growth of the CNTs is commonly observed. For plasma-enhanced CCVD lower temperatures are needed and highly aligned CNTs are obtained but mostly multiwalled CNTs are formed.[18]

A new approach in this field is CCVD assisted by inductive heating.[13] Inductive heating is clean, easy to set up, and an inexpensive method. In contrast to conventional heating high temperatures are generated within the carrier material or catalyst instead by convection from outside. Because of this reverse temperature gradient thinner carbon nanotubes are created that grow faster than those thicker ones commonly formed.[21] For the rapid synthesis of carbon nanotubes by inductive heating small silicon chips are used that are electroplated with a nickel and chromium layer.[22] Importantly, inductive heating allows reaching the required temperature above 700 °C very rapidly. The heating method allows control of the diameter, because higher temperatures give thinner carbon nanotubes. The average diameter can be controlled from 6.8 to 8.0 nm simply by lowering the power input.

A large-scale approach was achieved by Lupu et al. using a metal rod which was electrochemically oxidized to give a porous surface on which the catalyst was dispersed. Different types of CNTs were produced with different types of catalyst based on Fe and/or Co. CNTs were prepared by inductive heating at temperatures between 600 and 1000 °C.[13]

Inductive heating leads to much faster heating and cooling and thus shorter overall reaction times. Furthermore, the inductive-heating-assisted CCVD allows lowering of the energy consumption by two to three times, because heating is restricted to the area where the synthesis takes place.

Recently, ring-shaped, microstructured (between 600 to 1500 μm diameter) copper on silicon was employed for inductive heating. The ring shape of the copper allowed induction of Joule's heating and rapid temperature rise occurs in a very localized area. Several of these microstructures can simultaneously be used with one inductor.[18]

Magnetic Fluid Hyperthermia in the Treatment of Cancer.

The second most frequent cause of death worldwide after cardiovascular disease is cancer. Due to a longer life probability the cancer risk will increase in the future. In spite of great medical and scientific efforts in the last decades many cancer types still have a high mortality rate.[23] Therefore, the development of more efficient cancer therapies is still one of the most predominant medical tasks in our civilization.

In addition to standard treatment such as chemotherapy and radiation therapy, resection hyperthermia has recently been investigated as a new option in cancer therapy. Hyperthermia, also called thermal therapy or thermotherapy, is a medical application in which body tissue is exposed to high temperatures (40–45 °C) by external physical action.[24] Tumor tissue is more sensitive to hyperthermia because of inferior blood supply and a lower thermal resistance compared to healthy tissue. In clinical studies it was shown that the increase of the temperature in the cell leads to several physiological effects. Temperatures above 42 °C have a direct cytotoxic effect in the case of prolonged exposure. Furthermore, a temperature between 40–42 °C induces protein denaturation, which leads to damage at cell membranes, in the mitotic S-phase and in structural alterations of enzyme involved in DNA synthesis and repair. An additional important clinical aspect of hyperthermia is the increased expression of heat shock protein.[25] Currently, oncologists often use hyperthermia cancer treatment in combination with radiotherapy and chemotherapy. In addition to the elimination of many cancerous cells, hyperthermia can make resistant cells more vulnerable to other treatments.[26] Three technical concepts are commonly pursued: a) the whole-body hyperthermia, b) the localized hyperthermia, and c) the regional hyperthermia. Heating can be generated with radio and microwave frequencies as well as with laser wavelengths. An important parameter in this context is the specific absorption rate (SAR) (eq 12).

$$SAR = C\frac{\Delta T}{\Delta t}\frac{1}{m} \tag{12}$$

It is a measure of the rate at which the energy is absorbed by the body, where C is the specific heat of the material and m the total weight of the material. These procedures have frequently the disadvantage of an inhomogeneous heating in the target tissue, because the specific heat is not homogeneous. The power absorption depends on electronic properties of the tissue (e.g., bones and muscles). Also healthy tissue can be damaged by dispersion. This is especially a problem for therapy of deep-seated tumors. This limitation can be conquered by magnetic fluid hyperthermia treatment (MFH). In this technique magnetic nanoparticles, which are injected into the target region, are selectively heated in an externally applied AC magnetic field. The first systematic concept studies were performed in 1993 by Jordan et al.[27] and proved the safety and the effectiveness in preclinical and clinical investigations.[28] Inductive heating is a contact-free heating method. The direct coupling of nanoparticles with the magnetic field and the knowledge on the individual values for the specific heat C, inductive heating can well be controlled in this context.

Jordan et al. utilized dispersions of superparamagnetic iron oxide particles in water with an iron concentration of 112 $mg\,mL^{-1}$.[29] The nanoparticles are composed of an iron oxide core (magnetite) with an average diameter of 15 nm with an aminosilane shell. This coating guarantees an improved biocompatibility and the residence time in the tumor cells. Due to the great resistance to body tissues, the combination with other treatments is possible. The heating occurs in a magnetic field applicator (MFH® 300F, MagForce) with a 100 kHz alternating magnetic field and with a field amplitude of 2–15 $kA\,m^{-1}$ (corresponding to 15–20 mT).[30] It was demonstrated, that 3 mL of the magnetic fluid in a 60 mL tumor volume yields SAR values of $>500\,W\,kg^{-1}$. This power density is much higher compared to external heating methods such as regional hyperthermia (30–50 $W\,kg^{-1}$).

Prior to treatment the injected amount of ferrofluid was analyzed by medical applications (MRT, ultrasonic) based on the tumor volume. The administration of the nanoparticles was carried out by direct, punctured injection and the nanoparticle density was mapped using CT imaging. Because of the density, the SAR of the nanoparticles, and the estimated perfusion within the tumor area, the magnetic field strength was set individually until the calculated temperature was reached. The patients received 6–8 hyperthermia treatments over a period of one hour. For the first session the temperature measurements were conducted with a thermometry catheter deposited in the tumor to precisely reach the calculated temperature. In phase-II of treatment patients underwent a recurrent glioblastoma multiform, a most aggressive malignant primary brain tumor. The survival rate of patients was doubled from 6.2 to 13.4 months.[31,32]

Besides superparamagnetic iron oxide nanoparticles several other magnetic nanomaterials such as iron–palladium and cobalt, ferrimagnetic spinels, cobalt ferrite, Mn–Zn and Mn–Zn–Gd ferrite particles, copper–nickel, ferromagnetic perovskites $La_{1-x}Sr_xMnO_3$, $Ni_{(1-x)}Cr_x$, gadolinium-, calcium-, and lanthanum complexes, and ferrimagnetic $SrFe_{12}O_{19}/\gamma\text{-}Fe_2O_3$ composites were tested for hyperthermia applications.[9,33,34]

Recently, the development of multipurpose systems based on hyperthermia have been discussed,[35] e.g. by using the heat to releases a drug in the target area. Also particles with an antibody-modified targeting shell for the selective adhesion to the tumor tissue were investigated.[36] It needs to be pointed out that administering sufficient amounts of particles inside the tumor tissue is still one major problem. Often it is still too low for an effective hyperthermia treatment.

♦ *Inductive Heating in Organic Synthesis*

General Considerations.

Despite the fact that inductive heating has been introduced in domestic kitchens more than a decade ago, this enabling heating technology has hardly reached the chemical laboratories yet. Likewise, microwave heating had a similar sluggish move into the world of chemistry two decades ago although we all had used appropriate kitchenware much longer. Only in 2008, we introduced the application of magnetic induction as a heating technology in combination with flow devices in organic synthesis.[9]

The Setup.

As described above, heating by electromagnetic induction can rely on different physical effects. For example, heating can be generated in superparamagnetic nanoparticles based on Fe_2O_3/Fe_3O_4 that are coated with silica gel. In comparison with other materials MagSilica® (Fe_2O_3/Fe_3O_4 core with SiO_2 shell) performed best in heating studies, when an oscillating electromagnetic field was employed externally (Figure 4).

As described above, heating by electromagnetic induction can rely on different physical effects. Thus, heating can be generated in superparamagnetic nanoparticles based on

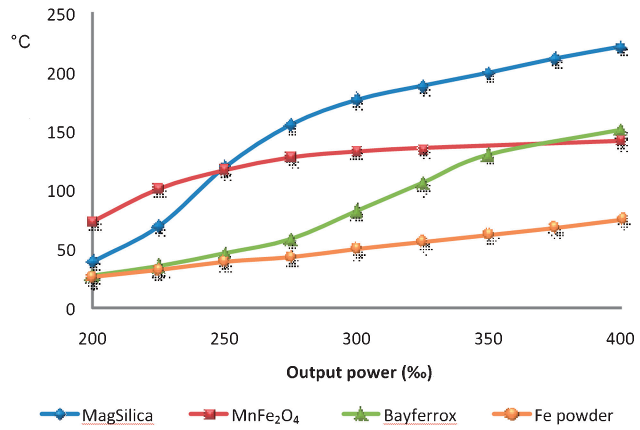

Figure 4. Heating profile of MagSilica®, $MnFe_2O_4$, Bayferrox®, and iron powder.

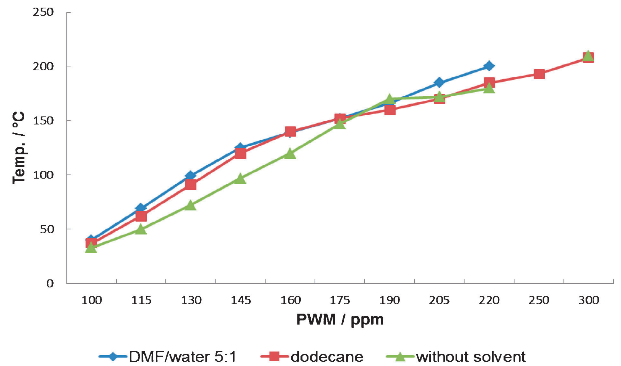

Figure 5. Heating profile of copper wire, measured without solvent, with degassed dodecane and with degassed DMF/water (5:1) at a frequency of 15 kHz (PWM: output power in ppm).

Fe_2O_3/Fe_3O_4 that are coated with silica gel. Likewise, conductive materials, commonly these are metals such as steel or copper, heat up in the presence of an externally applied electromagnetic field. Ideally, these materials can serve as fixed bed materials inside flow devices particularly in microreactors.

Likewise, conductive materials, commonly these are metals such as steel or copper, heat up in the presence of an externally applied oscillating electromagnetic field. Copper wire shows conductive properties and the heating profile of copper turnings/wire inside a PEEK or glass reactor clearly reveals that solvents can be heated up to 200 °C at low power input (Figure 5).[37]

Ideally, all these materials can serve as fixed bed materials inside flow devices particularly in microreactors.[38] Indeed, continuous flow processes using miniaturized flow reactors have seen great interest in the organic community for a bit more than a decade.[39] From established industrial processes it is well established that continuous flow processes guarantee constant reaction parameters (temperature, time, amount of reagents and solvents, efficient mixing, etc.).[40] With respect to thermal and mass transfer, efficient mixing as well as mass transport can be controlled much better compared to the corresponding batch processes. Continuous flow reactors are generally smaller than batch reactors. Still, even bench-sized reactors are capable of producing more product in a given time than an analogous batch reactor.[41]

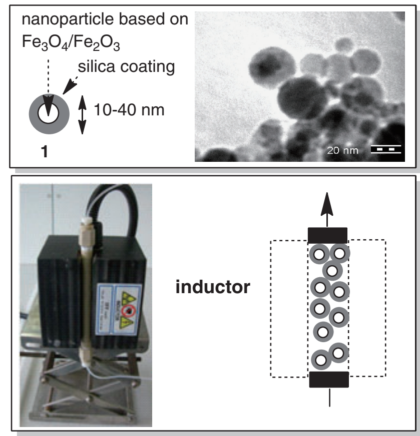

Figure 6. Schematic presentation (top right) and TEM micrograph (topright) of MagSilica®. Flow reactor filled with magnetic nanoparticles (bottom left) and PEEK reactor encased with an inductor (bottom right).

In contrast to microwave irradiation that can interact with a wide range of (reactor) materials as well as reactants and solvents, inductive heating is very specific. Here, only conductive or superparamagnetic materials are heated, which simplifies the technical set up of a flow system to a great extent. Thus, fewer parameters have to be considered and temperature control is simplified.

Glass or high-performance polymers such as poly(ether ether ketone) (PEEK) are suited as reactor material. For high-temperature transformations where reactions are conducted above the boiling point of the solvent also ceramic reactors can be envisaged which in addition are equipped with an in line back pressure regulator. The reactor filled with the inductively heatable fixed bed material is encased by an inductor as shown in Figure 6. A closed chamber as needed in microwave applications is not required.

Comparison of Heating Modes.

The high-temperature sigmatropic Claisen rearrangement of allyl aryl ether **2** to phenol **3** was used to compare the efficiency of three heating concepts: a) conventional heating in an oil bath, b) microwave heating, and c) inductive heating under batch conditions. This reaction was chosen because it only proceeds with moderate yield at high temperature in an oil bath (Scheme 1). We regarded this to be a prerequisite for such a study. Both heating methods, microwave as well as electromagnetic radiation, performed superior to conventional heating and gave similar results concerning reaction times and degree of transformation. Certainly, one cannot expect a special effect exerted by electromagnetic irradiation. The inductive heating simply provides a very rapid and efficient way of heating. The major obstacle to properly compare the three techniques is the difficulty to determine the exact temperature of superparamagnetic nanoparticles when exposed to electromagnetic irradiation. However, this is a general problem for "indirect" heating techniques and has therefore also been discussed in the field of microwave-irradiated reactions.[42]

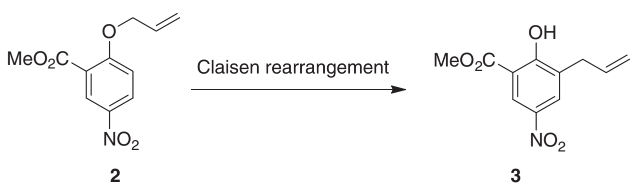

	oil bath	μw heating	inductive heating
Conditions	200 °C, toluene, 120 min,	SiC, 200 °C, toluene, 120 min	25 kHz, 200 °C, MagSilica, toluene, 120 min
Yield/%	17	38	39

Scheme 1. Comparison between conventional heating (external oil bath), microwave irradiation and inductive heating under batch conditions.

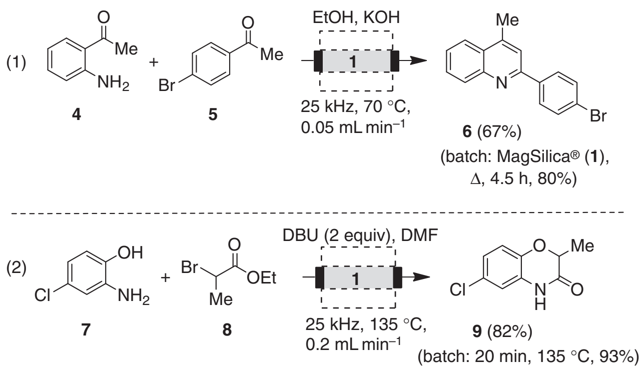

Scheme 2. Continuous-flow synthesis of heterocycles.

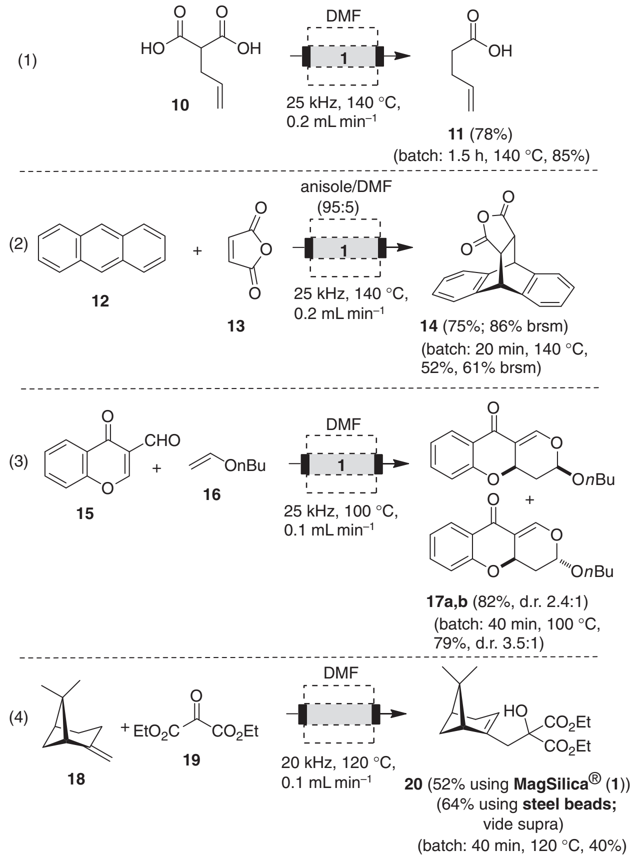

Scheme 3. Pericyclic continuous flow reactions.

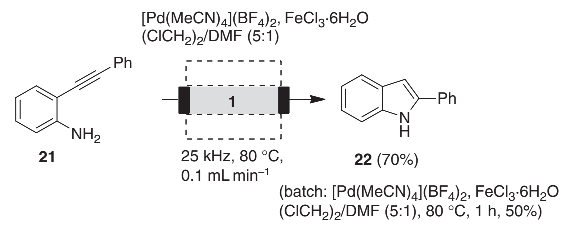

Scheme 4. Palladium-catalyzed inductively heated hydroamination of aryl alkyne **21**.

◆ *Synthetic Applications*

Synthesis with Iron Oxide Nanoparticles.

A key issue when using core–shell iron oxide nanoparticles as inductively heatable solids in organic synthesis is their chemical stability (Scheme 2). How inert is the silica shell in the presence of a wide range of conditions at very high temperatures present at the interface between silica shell and reaction mixtures? Particularly strongly aqueous acidic and basic conditions as well as polar solvents such as water, DMSO, DMF, etc. have to be considered as destructive toward the silica protection.

Another group of reactions studied are pericyclic reactions such as decarboxylations, cycloadditions to cycloadducts **14** and **17** as well as the Alder-ene reaction yielding terpenoid **20** (Scheme 3, Entries 1–4). In the majority of cases the inductive heating combined with flow turned out to be superior to conventional batch type processes in the flask. Here, reaction times and/or isolated yields were taken as criteria for comparison.

MagSilica® nanoparticles can also be employed under conditions of Pd-catalysis. Intramolecular hydroamination of alkyne **21** gave indol derivative **22** in significantly higher yield than found under batch mode conditions (Scheme 4).

Oxidations with Inductively Heated Solid Metal Oxides.

Oxidations are highly important processes, particularly in the industrial context. It was shown, that solid-phase oxidations[43] can be performed by mixing different solid oxidants like MagTrieve™ (CrO_2) or nickel peroxide (NiO_2) with MagSilica®. These mixed fixed beds remain solid as the oxidation proceeds under inductive heating conditions. This setup minimizes the issue of metal contamination. Several oxidations were achieved including oxidations of alcohols **23** and **25** (Scheme 5, Entries 1 and 2), and anthracene **27** (Scheme 5, Entry 3).

Likewise, the combination of MagSilica® and nickel peroxide allowed dehydration of coumarin **29** as well as the oxidation of benzyl amine **31** to nitrile **32** (Scheme 6).

Inductive Heating with Conductive Metals.

As summarized in Section **2** also conductive materials such as copper or steel heat up in an oscillating electromagnetic field. The heating effect is created through eddy currents and resistance in the material results in Joule's heating.

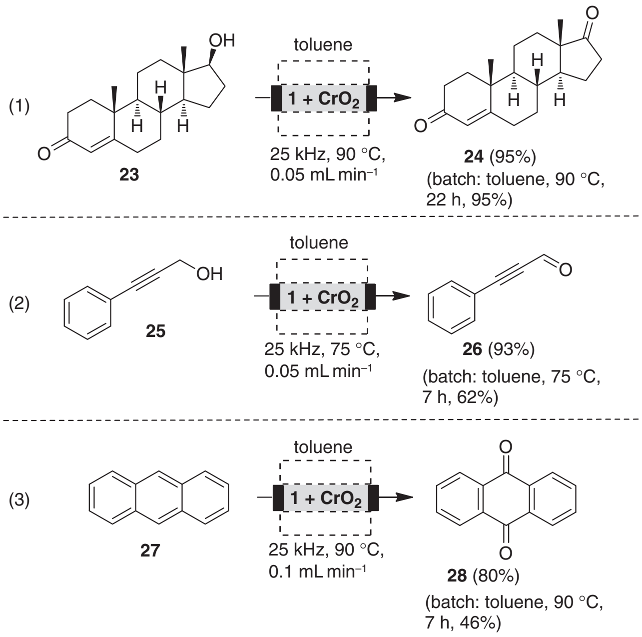

Scheme 5. Continuous CrO_2-promoted flow oxidations under inductive heating conditions.

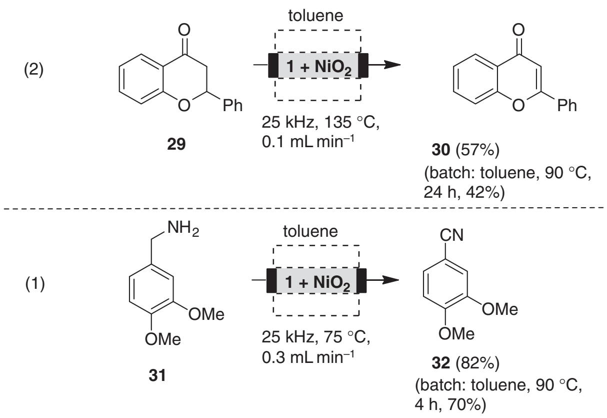

Scheme 6. Continuous NiO_2-promoted flow oxidations under inductive heating conditions.

Steel beads (0.8 mm diameter) have served as fixed bed materials of flow reactors. Smaller steel beads (0.4 mm) were less efficiently heated or bigger ones (2.0 mm) were too large to create a large hot surface area inside the reactor. The combination of inductive heating with steel beads and flow chemistry was beneficially employed for conducting several multicomponent reactions (MCR).[44] Typical examples are the asymmetric Mannich reaction at elevated temperature using L-proline as catalyst affording β-amino ketone **36** (Scheme 7, Entry 1), the Biginelli reaction furnishing tetrahydropyrimidine **40** (Entry 2) and the Petasis reaction, a variant of the Mannich reaction that provides amines **44** and **47** (Entries 3 and 4) that all proceeded with excellent yields.

Steel beads also served as a source of heat to conduct the palladium-catalyzed two-step tandem reaction composed of a Sonogashira–Hagihara reaction followed by a 5-*endo* dig cyclization to yield benzofuran **50** (Scheme 8).

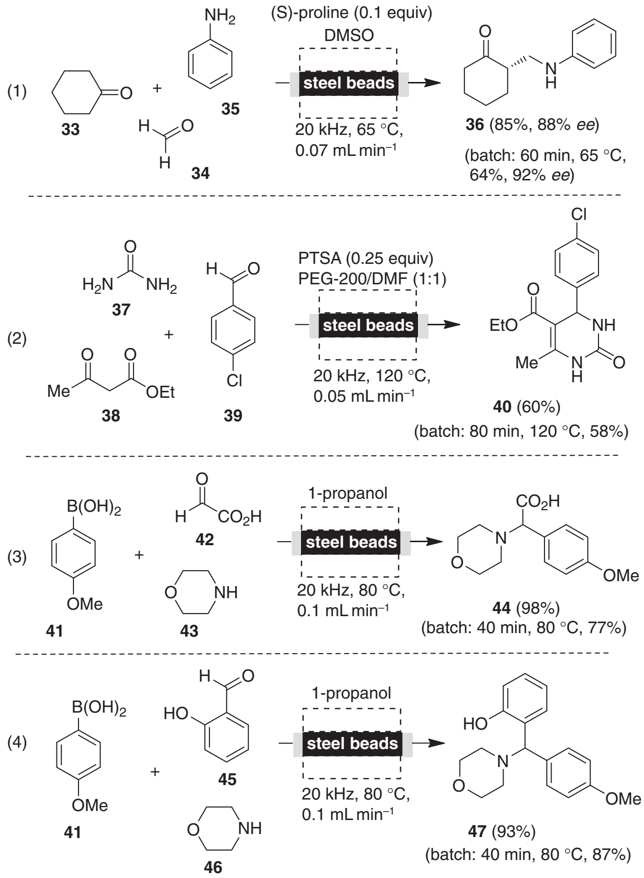

Scheme 7. Inductively heated continuous-flow multicomponent reactions.

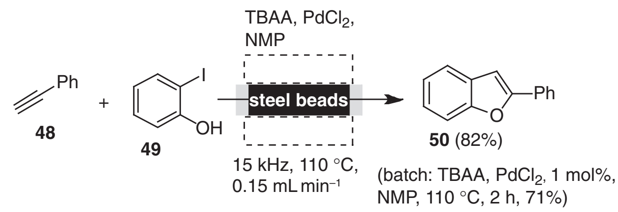

Scheme 8. Palladium-catalyzed inductively heated cyclization under flow conditions.

Also copper wire is efficiently heated in an oscillating electromagnetic field. In this environment, copper heats up to a point that it can also act as a catalyst in several transformations. Thus, the Huisgin "click" cycloaddition becomes possible after in situ formation of the alkyl azide yielding triazoles like **53** (Scheme 9, Entry 1). High-temperature copper also acts as catalyst in the decarboxylation of propargylic carboxylic acid **54** under flow conditions to afford propargyl(2-propynyl) alcohol **55** (Scheme 9, Entry 2). Third, copper-mediated cyclization of aryl carboxylic acid **56** are possible under flow conditions (Scheme 9, Entry 3).

As an extension, the multistep flow synthesis of vinyl azides and their application in the synthesis of vinyltriazoles was conducted.[45] First, a polymer-bound equivalent of iodine azide yielded a 2-iodoazide starting from alkene **58**. The iodoazide

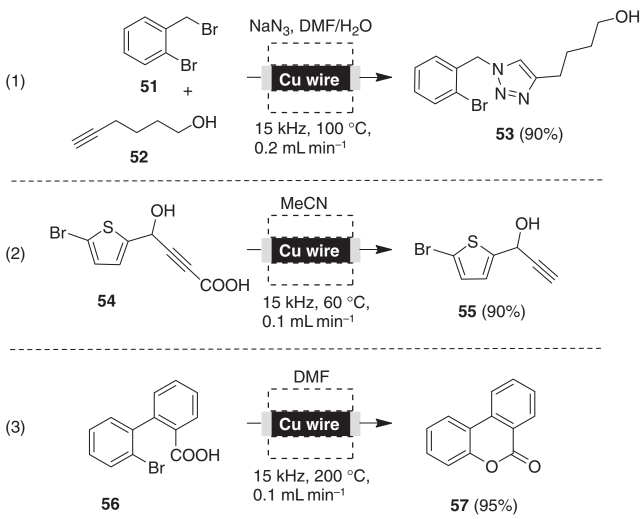

Scheme 9. Continuous copper-catalyzed Huisgen "click" cycloaddition, decarboxylation, and cyclization by inductive heating.

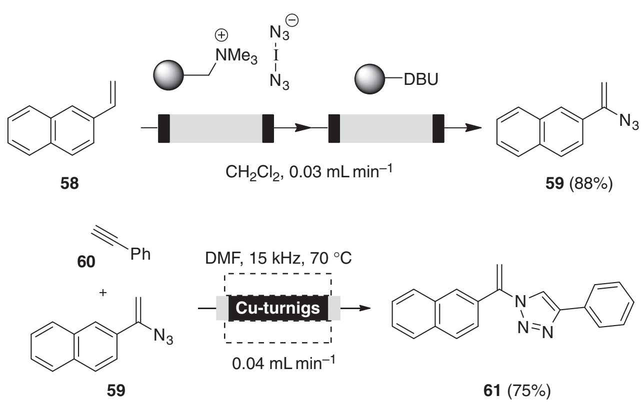

Scheme 10. Continuous two-step synthesis of vinylazides followed by copper-catalyzed Huisgen "click" cycloaddition.

was directly pumped into a second reactor loaded with polymer-bound DBU, thus mediating an elimination step under flow conditions. This two-step flow protocol yielded vinylazide **59** in very good yield. The third step involved the formation of vinyltriazoles **61** by the copper-catalyzed Huisgen "click" cycloaddition. Again, the required heat was generated by an oscillating electromagnetic field that was exposed to copper turnings (Scheme 10).

Synthesis with Functionalized Iron Oxide Nanoparticles.

The primary role of the silica shell in the core–shell particles is to keep the iron oxide nanoparticles apart from each other. Otherwise there is a tendency of clustering with subsequent loss of the superparamagnetic properties. In addition, the silica shell of MagSilica® can be modified and functionalized based on known methods. For example, palladium nanoparticles were immobilized on these core–shell particles and this doped superparamagnetic material **62** was used as heatable and

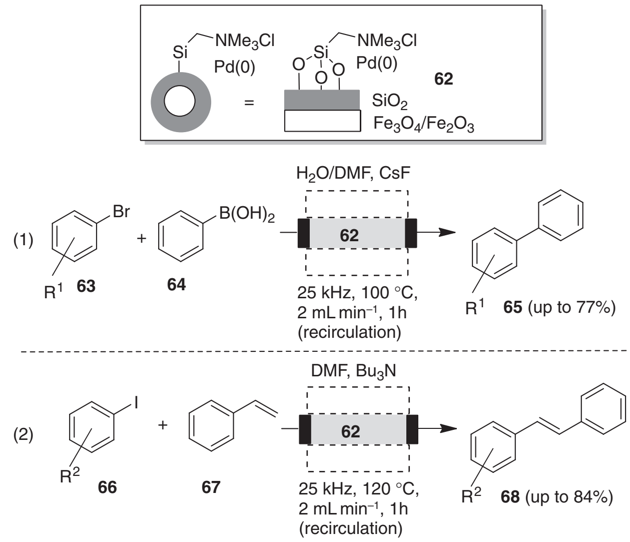

Scheme 11. Inductively heated immobilized Pd-catalyzed C–C-coupling reactions under flow conditions.

catalytically active fixed bed material in flow reactors. In fact, this catalytic system can be employed to carry out Suzuki and Heck cross-coupling reactions to yield products of type **65** and **68**, respectively (Scheme 11). In principal recyclability is an advantage of such heatable heterogeneous catalysts. However, the catalytic system lost its activity after three runs despite the fact that leaching was low (Entry 1: 34 ppm for Pd; Entry 2: 100 ppm for Pd).

♦ *Conclusion*

The use of inductively heated iron oxide nanoparticles has found first use in the treatment against solids tumors. Only recently, the superparamagnetic properties of these nanoparticles has been exploited as a heating technology in organic synthesis. As far as efficacy is concerned inductive heating is comparable with microwave irradiation. However, many of the safety issues associated with microwave irradiation do not exist, making inductive heating an attractive new heating method in organic synthesis. Ideally inductive heating can be combined with microreactors creating powerful new synthetic platforms.

From our experience, the technical setup is much simpler than corresponding microwave devices when performing chemistry under flow conditions. Also leaching of metal species is minimal and in-line scavengers can be applied if necessary. Furthermore, the reactor concept is simple and can be adapted to other flow systems too. In view of the dramatic increase of interest in flow chemistry we believe that this new heating technology has future prospects both in academia and in industry.

Our contributions in this field were supported by the Fonds der Chemischen Industrie and the Ministry of Science and Culture of Lower Saxony (MWK). We thank Henkel AG & KGaA (Düsseldorf, Germany), EVONIK Degussa GmbH (Essen, Germany), and IFF GmbH (München, Germany) for financial or technical support.

References and Notes

1 a) C. O. Kappe, *Angew. Chem., Int. Ed.* **2004**, *43*, 6250. b) P. Lidström, J. Tierney, B. Wathey, J. Westman, *Tetrahedron* **2001**, *57*, 9225.

2 G. Benkowsky, *Induktionserwärmung: Härten, Glühen, Schmelzen, Löten, Schweißn: Grundlagen und praktische Anleitungen für Induktionserwärmungsverfahren, insbesondere auf dem Gebiet der Hochfrequenzerwärmung*, 5th ed., Verlag Technik, Berlin, **1990**, p. 12.

3 D. Liedtke, *Wärmebehandlung von Eisenwerkstoffen I: Grundlagen und Anwendungen*, Expert-Verlag, Renningen, **1991**.

4 a) J. M. Matesa, K. J. Won, H. M. Demarest, Jr., U.S. Patent 4,610,711, **1986**. b) Forschungsverbund Berlin e. V., Patent DE 196 38 966 A 1, **1997**. c) Sunicon AG, Patent DE 10 2009 035 041, **2011**.

5 a) C. Lammel, K. Dilger, *Adhäs.—Kleben Dichten* **2000**, *44*, 11. b) S. Wlach, G. Wachinger, T. Meer, C. Lammel, WO/2009/047010, PCT/EP2008/008664, **2009**. c) T. R. Peterson, M. A. Walker, U.S. Patent 5,486,684, **1996**.

6 V. Sechovský, in *Encyclopedia of Materials: Science and Technology*, ed. by K. H. J. Buschow, R. W. Cahn, M. C. Flemings, B. Ilschner, E. J. Kramer, S. Mahajan, P. Veyssière, Elsevier, Amsterdam, **2001**, p. 5021. doi:10.1016/B0-08-043152-6/00872-X.

7 See for data: V. Rudnev, D. Loveless, R. L. Cook, M. Black, *Handbook of Induction Heating*, Marcel Dekker Inc., New York, **2003**, p. 113.

8 A.-H. Lu, E. L. Salabas, F. Schüth, *Angew. Chem.* **2007**, *119*, 1242.

9 S. Ceylan, C. Friese, C. Lammel, K. Mazac, A. Kirschning, *Angew. Chem., Int. Ed.* **2008**, *47*, 8950.

10 S. Laurent, S. Dutz, U. O. Häfeli, M. Mahmoudi, *Adv. Colloid Interface Sci.* **2011**, *166*, 8.

11 a) J.-P. Fortin, F. Gazeau, C. Wilhelm, *Eur. Biophys. J.* **2008**, *37*, 223. b) M. S. Islam, J. Kurawaki, Y. Kusumoto, M. Abdulla-Al-Mamun, M. Z. B. Mukhlish, *J. Sci. Res.* **2012**, *4*, 99.

12 R. E. Rosensweig, *J. Magn. Magn. Mater.* **2002**, *252*, 370.

13 D. Lupu, A. R. Biriş, A. Jianu, C. Bunescu, E. Burkel, E. Indrea, G. Mihăilescu, S. Pruneanu, L. Olenic, I. Mişan, *Carbon* **2004**, *42*, 503.

14 S. Iijima, *Nature* **1991**, *354*, 56.

15 W. Z. Li, S. S. Xie, L. X. Qian, B. H. Chang, B. S. Zou, W. Y. Zhou, R. A. Zhao, G. Wang, *Science* **1996**, *274*, 1701.

16 a) R. H. Baughman, A. A. Zakhidov, W. A. de Heer, *Science* **2002**, *297*, 787. b) Y. Soneda, L. Duclaux, F. Béguin, *Carbon* **2002**, *40*, 965.

17 T. Gennet, A. C. Dillon, J. L. Alleman, K. M. Jones, P. A. Parilla, M. J. Heben, *Mater. Res. Soc. Symp. Proc.* **2000**, *633*, A2.3.

18 B. D. Sosnowchik, L. Lin, *Nano/Micro Engineered and Molecular Systems, 2007. NEMS '07. 2nd IEEE International Conference*, **2007**, pp. 866–871.

19 E. Couteau, K. Hernadi, J. W. Seo, L. Thiên-Nga, Cs. Mikó, R. Gaál, L. Forró, *Chem. Phys. Lett.* **2003**, *378*, 9.

20 a) V. Ivanov, J. B. Nagy, Ph. Lambin, A. Lucas, X. B. Zhang, X. F. Zhang, D. Bernaerts, G. Van Tendeloo, S. Amelinckx, J. Van Landuyt, *Chem. Phys. Lett.* **1994**, *223*, 329. b) K. Hernadi, A. Fonseca, P. Piedigrosso, M. Delvaux, J. B. Nagy, D. Bernaerts, J. Riga, *Catal. Lett.* **1997**, *48*, 229. c) K. Hernadi, A. Fonseca, J. B. Nagy, D. Bemaerts, A. Fudala, A. A. Lucas, *Zeolites* **1996**, *17*, 416.

21 K. P. de Jong, J. W. Geus, *Catal. Rev., Sci. Eng.* **2000**, *42*, 481.

22 B. D. Sosnowchik, L. Lin, *Appl. Phys. Lett.* **2006**, *89*, 193112.

23 A. Jemal, F. Bray, M. M. Center, J. Ferlay, E. Ward, D. Forman, *Ca-Cancer J. Clin.* **2011**, *61*, 69.

24 J. van der Zee, *Ann. Oncol.* **2002**, *13*, 1173.

25 A. Ito, F. Matsuoka, H. Honda, T. Kobayashi, *Cancer Gene Ther.* **2003**, *10*, 918.

26 P. P. Wust, B. Hildebrandt, G. Sreenivasa, B. Rau, J. Gellermann, H. Riess, R. Felix, P. M. Schlag, *Lancet Oncol.* **2002**, *3*, 487.

27 A. Jordan, P. Wust, H. Fähling, W. John, A. Hinz, R. Felix, *Int. J. Hyperthermia* **1993**, *9*, 51.

28 a) A. Jordan, R. Scholz, K. Maier-Hauff, M. Johannsen, P. Wust, J. Nadobny, H. Schirra, H. Schmidt, S. Deger, S. Loening, W. Lanksch, R. Felix, *J. Magn. Magn. Mater.* **2001**, *225*, 118. b) B. Thiesen, A. Jordan, *Int. J. Hyperthermia* **2008**, *24*, 467. c) M. Johannsen, U. Gneveckow, B. Thiesen, K. Taymoorian, C. H. Cho, N. Waldöfner, R. Scholz, A. Jordan, S. A. Loening, P. Wust, *Eur. Urol.* **2007**, *52*, 1653.

29 The particles are named NanoTherm® and are manufactured by MagForce.

30 U. Gneveckow, A. Jordan, R. Scholz, V. Brüß, N. Waldöfner, J. Ricke, A. Feussner, P. Wust, B. Hildebrandt, B. Rau, *Med. Phys.* **2004**, *31*, 1444.

31 A. C. Silva, T. R. Oliveira, J. B. Mamani, S. M. F. Malheiros, L. Malavolta, L. F. Pavon, T. T. Sibov, E. Amaro, Jr., A. Tannús, E. L. G. Vidoto, M. J. Matins, R. S. Santos, L. F. Gamarra, *Int. J. Nanomed.* **2011**, *6*, 591.

32 R. Hergt, W. Andra, C. G. d'Ambly, I. Hilger, W. A. Kaiser, U. Richter, H.-G. Schmidt, *IEEE Trans. Magn.* **1998**, *34*, 3745.

33 I. Sharifi, H. Shokrollahi, S. Amiri, *J. Magn. Magn. Mater.* **2012**, *324*, 903.

34 R. Epherre, E. Duguet, S. Mornet, E. Pollert, S. Louguet, S. Lecommandoux, C. Schatz, G. Goglio, *J. Mater. Chem.* **2011**, *21*, 4393.

35 D.-L. Zhao, H.-L. Zhang, X.-W. Zeng, Q.-S. Xia, J.-T. Tang, *Biomed. Mater.* **2006**, *1*, 198.

36 a) A. M. Wu, P. D. Senter, *Nat. Biotechnol.* **2005**, *23*, 1137. b) R. V. J. Chari, *Acc. Chem. Res.* **2008**, *41*, 98. c) S. C. Alley, N. M. Okeley, P. D. Senter, *Curr. Opin. Chem. Biol.* **2010**, *14*, 529.

37 S. Ceylan, T. Klande, C. Vogt, C. Friese, A. Kirschning, *Synlett* **2010**, 2009.

38 Reviews on flow reactors: a) V. Hessel, *Chem. Eng. Technol.* **2009**, *32*, 1655. b) K. Geyer, T. Gustafsson, P. H. Seeberger, *Synlett* **2009**, 2382. c) R. L. Hartman, K. F. Jensen, *Lab Chip* **2009**, *9*, 2495. d) X. Y. Mak, P. Laurino, P. H. Seeberger, *Beilstein J. Org. Chem.* **2009**, *5*, No. 19. doi:10.3762/bjoc.5.19. e) C. Wiles, P. Watts, *Eur. J. Org. Chem.* **2008**, 1655. f) T. Fukuyama, Md. T. Rahman, M. Sato, I. Ryu, *Synlett* **2008**, 151. g) B. Ahmed-Omer, J. C. Brandt, T. Wirth, *Org. Biomol. Chem.* **2007**, *5*, 733. h) P. Watts, C. Wiles, *Chem. Commun.* **2007**, 443. i) B. P. Mason, K. E. Price, J. L. Steinbacher, A. R. Bogdan, D. T. McQuade, *Chem. Rev.* **2007**, *107*, 2300. j) J. Kobayashi, Y. Mori, S. Kobayashi, *Chem.—Asian J.* **2006**, *1*, 22. k) W. Verboom, *Chem. Eng. Technol.* **2009**, *32*, 1695. l) J. P. McMullen, K. F. Jensen, *Annu. Rev. Anal. Chem.* **2010**, *3*, 19. m) K. Tanaka, K. Fukase, *Org. Process Res. Dev.* **2009**, *13*, 983. n) D. M. Roberge, B. Zimmermann, F. Rainone, M. Gottsponer, M. Eyholzer, N. Kockmann, *Org. Process Res. Dev.* **2008**, *12*, 905. o) G. Jas, A. Kirschning, *Chem.—Eur. J.* **2003**, *9*, 5708. p) A. Kirschning, G. Jas, in *Immobilized Catalysts: Solid Phases, Immobilization and Applications* in *Topics in Current Chemistry*, ed. by A. Kirschning, Springer-Verlag, Berlin, **2004**, Vol. 242, pp. 209–239. doi:10.1007/b96877. q) I. R. Baxendale, S. V. Ley, in *New Avenues to Efficient Chemical Synthesis: Emerging Technologies*, ed. by P. H. Seeberger, T. Blume, Springer, Berlin, Heidelberg, **2007**, pp. 151–185. doi:10.1007/2789_2007_033. r) S. Ceylan, A. Kirschning, in *Recoverable and Recyclable Catalysts*, ed. by M. Benaglia, John Wiley & Sons, Ltd., **2009**, Chap. 13, p. 379. s) J.-i. Yoshida, A. Nagaki, T. Yamada, *Chem.—Eur. J.* **2008**, *14*, 7450. t) J. P. McMullen, K. F. Jensen, *Annu. Rev. Anal. Chem.* **2010**, *3*, 19. u) D. Webb, T. F. Jamison, *Chem. Sci.* **2010**, *1*, 675. v) J. Wegner, S. Ceylan, A. Kirschning, *Adv. Synth. Catal.* **2012**, *354*, 17. w) W.-Y. Lin, Y. Wang, S. Wang, H.-R. Tseng, *Nano Today* **2009**, *4*, 470. x) G. M. Whitesides, *Nature* **2006**, *442*, 368. y) A. J. deMello, *Nature* **2006**, *442*, 394. z) H. Song, D. L. Chen, R. F. Ismagilov, Angew. Chem. **2006**, *118*, 7494; H. Song, D. L. Chen, R. F. Ismagilov, *Angew. Chem., Int. Ed.* **2006**, *45*, 7336.

39 See for example: K. Geyer, J. D. C. Codée, P. H. Seeberger, *Chem.—Eur. J.* **2006**, *12*, 8434.

40 A. Kirschning, W. Solodenko, K. Mennecke, *Chem.—Eur. J.* **2006**, *12*, 5972.

41 a) *Handbook of Micro Reactors*, ed. by V. Hessel, J. C. Schouten, A. Renken, Y. Wang, J.-i. Yoshida, Wiley-VCH, Weinheim, **2009**. b) V. Hessel, P. Löb, H. Löwe, in *Microreactors in Organic Synthesis and Catalysis*, ed. by T. Wirth, Wiley-VCH, Weinheim, Germany, **2008**, Chap. 5, pp. 211–275. c) N. Kockmann, M. Gottsponer, B. Zimmermann, D. M. Roberge, *Chem.—Eur. J.* **2008**, *14*, 7470.

42 a) C. O. Kappe, D. Dallinger, *Mol. Diversity* **2009**, *13*, 71. b) S. Caddick, R. Fitzmaurice, *Tetrahedron* **2009**, *65*, 3325. c) M. Matsuzawa, S. Togashi, S. Hasebe, *J. Therm. Sci. Technol.* **2012**, *7*, 58.

43 J. Wegner, S. Ceylan, C. Friese, A. Kirschning, *Eur. J. Org. Chem.* **2010**, 4372.

44 S. Ceylan, L. Coutable, J. Wegner, A. Kirschning, *Chem.—Eur. J.* **2011**, *17*, 1884.

45 L. Kupracz, J. Hartwig, J. Wegner, S. Ceylan, A. Kirschning, *Beilstein J. Org. Chem.* **2011**, *7*, 1441.

